Laser and Particle Beams (2011), *29*, 69–80.

doi:10.1017/S0263034610000777

Theoretical and experimental studies of material radiative properties and their applications to laser and heavy ion inertial fusion

N. YU. ORLOV,[1] O.B. DENISOV,[1] O.N. ROSMEJ,[2] D. SCHÄFER,[3] TH. NISIUS,[3] TH. WILHEIN,[3] N. ZHIDKOV,[4] A. KUNIN,[4] N. SUSLOV,[4] A. PINEGIN,[4] V. VATULIN,[4] AND Y. ZHAO[5]

[1]Joint Institute for High Temperatures RAS, Institute for High Energy Density, Moscow, Russia
[2]GSI Helmholtzzentrum für Schwerionenforschung, Darmstadt, Germany
[3]RheinAhrCampus Remagen, Institute for X-optics, Remagen, Germany
[4]All Russian Scientific Research Institute of Experimental Physics, RFNC-VNIIEF, Sarov, Russia
[5]Institute of Modern Physics, CAS, Lanzhou, China

(RECEIVED 2 November 2010; ACCEPTED 3 December 2010)

Abstract

Theoretical and experimental studies of radiative properties of substances heated by pulsed current devises or lasers and used as X-ray sources have been carried out depending on plasma conditions, and specific spectra of X-ray absorption and radiation for different materials have been calculated. Important features of the theoretical model, known as the ion model of plasma, are discussed. This model can be applied for calculations of the radiative properties of complex materials over a wide range of plasma parameters. For purposes of indirect-driven inertial fusion based on the hohlraum concept, an optimization method is used for the selection of an effective complex hohlraum wall material, which provides high radiation efficiency at laser interaction with the wall. The radiation efficiency of the resulting material is compared with the efficiency of other composite materials that have previously been evaluated theoretically. A similar theoretical study is performed for the optically thin X-pinch plasma produced by exploding wires. Theoretical estimations of radiative efficiency are compared with experimental data that have been obtained from measurements of X-pinch radiation energy yield using two exploding wire materials, NiCr and Alloy 188. It is shown that the theoretical results agree well with the experimental data. A symmetric multilayer X-pinch, where W and Mo wires are used, is as well considered. The theoretical explanation of experimental phenomena is discussed based on the W and Mo radiative spectra. The ion model was as well applied for interpretation of experimental results on opacities of CHO-plasma obtained via indirect heating of low density polymer layers by means of soft X-rays. The new diagnostics method based on the deformation of the of the Carbon absorption K-edge when foam layer is heated to plasma is discussed. The spectral coefficients for X-ray absorption in CHO-plasma are calculated in the photon energy region around the Carbon K-edge for different plasma temperatures and mean foam density. In this case, the Carbon K-edge position on the energy scale can be used for plasma temperature diagnostic.

Keywords: Absorption K-edge; Foam targets; Hohlraum radiation; Indirect heating; Planck mean free paths; Radiative opacity; Rosseland; X-ray source

1. INTRODUCTION

The physics of inertial confinement fusion (ICF) is a field of very active research and requires fundamental studies of matter at high energy density. Theoretical and experimental investigations (Batani *et al.*, 2007; Bret & Deutsch, 2006; Gus'kov, 2005; Hora, 2007; Ng *et al.*, 2005; Sakagami *et al.*, 2006; Sasaki *et al.*, 2006; Someya *et al.*, 2006) provide progress in deep understanding of physical processes in matter, which is transformed into a high energy density state under heating and compression. The theoretical study of physical processes has to include (1) gas dynamics, (2) photon transport processes, (3) equation of state, (4) radiative opacities (Zeldovich & Raizer, 1966), which represent an important part of this study (Adamek *et al.*, 2006).

In the "indirect-driven" ICF scheme, hohlraums are used for efficient conversion of the laser energy into soft X-ray

Address correspondence and reprint requests to: N. Yu. Orlov, Joint Institute for High Temperatures RAS, Institute for High Energy Density, Izhorskaya. 13, Building 2, 125412, Moscow, Russia. E-mail: nyuorlov@mail.ru

(Lindl, 1998). The interaction of the radiation with the hohlraum wall is characterized by multiple absorption and reemission of X-rays. Part of the absorbed energy is lost due to the radiation heat transport into the wall. Increase of the wall opacity *via* optimization of the material composition leads to reduced radiation energy transfer and increases the hohlraum albedo, which is the ratio of reemitted to incident X-rays. Some peculiarities of indirectly driven ICF target designs were discussed in a previous publications (Denisov *et al.*, 2005; Borisenko *et al.*, 2003; Kilkenny *et al.*, 2005; Koresheva *et al.*, 2005; Kyrala *et al.*, 2005; Orlov *et al.*, 2007).

X-pinch plasma is a high brilliance SXR source produced by heating of two crossing X-shaped wires by a pulsed current of a high power driver (Zakharov *et al.*, 1982; Shelkovenko *et al.*, 2001; Zou *et al.*, 2006). X-pinch based X-ray source is characterized by high brightness and spatial stability for a wide range of wire materials, wire diameters, and current pulse parameters (Shelkovenko *et al.*, 2001). A modern scheme of so-called symmetric multilayer X-pinch was recently developed (Shelkovenko *et al.*, 2010).

The radiative characteristics of hohlraum wall plasmas and X-pinch plasmas depend on plasma temperature T, plasma densityρ, and plasma composition. The dependence of the radiative characteristics of the plasma on the X-ray source materials is one of the subjects of this paper. Another subject is connected with specific spectra of X-ray absorption and radiation for different materials.

The theoretical part of this paper gives a brief overview of different models used to calculate the radiative opacity of hot dense plasmas. Important features of the model used here are described. Two different physical approximations are proposed to estimate radiation efficiency for optically thick and optically thin plasmas. An optimizing procedure that can determine an effective complex material for producing optically thick plasma by laser interaction with a thick solid target is used. The radiation efficiency of the resulting material is compared with the efficiencies of different materials that have already been estimated theoretically (Suter *et al.*, 1999; Callahan-Miller & Tabak, 2000).

For optically thin plasmas, the Rosseland and Planck mean-free-paths are calculated for two exploding wire materials, NiCr and Alloy 188, at fixed temperature and different densities. Theoretical estimations of the X-ray source radiative efficiency are compared with experimental data on measurements of the X-pinch radiation energy yield. Theoretical discussion of the results is also presented. The next item is connected with a symmetric multilayer X-pinch, where tungsten W and molybdenum Mo wires are used (Shelkovenko *et al.*, 2010). Theoretical explanation of experimentally obtained phenomena is discussed based upon W and Mo radiative spectra.

In the next part of this paper, the theoretical approach, which was developed and used in previous studies, is applied to temperature diagnostics of low Z foams in combined laser — heavy ion beam experiments. The experimental goal is the investigation of the heavy ion stopping mechanism in ionized matter (Hoffmann *et al.*, 2005). Experiments require creating a plasma target, where dense homogeneous plasma can keep the temperature and density during further interaction with heavy-ion beam. This can be achieved by means of indirect-heating of polymer low density foams with hohlraum radiation.

For the characterization of temperature and ionization degree of indirect heated CHO-foams, measurements of photo-absorption K-edge energies in Carbon were used (Rosmej *et al.*, 2009). If the plasma temperature increases, the state of the whole ensemble of plasma atoms and ions is changed. It leads to the appearance of ions with higher ionization degrees and shifted to higher energies K-edge positions. The theoretical approach, which was used in previous items of this paper, gives, in particular, K-edge energies of different Carbon ions in ground and excited states and provides calculations of the spectral coefficients for X-ray absorption as well as the spectral characteristics of radiation transmitted through the CHO-plasma target. Comparison of the theoretical and experimental results (Rosmej *et al.*, 2009) is proposed to be used to estimate plasma temperature.

2. THEORETICAL APPROACH

Different theoretical models and corresponding computer codes have been developed to calculate spectral coefficients for X-ray absorption, the heat conductivity coefficients, Rosseland, and Planck mean free paths and other plasma characteristics. The density functional theory (March *et al.*, 1983; Rajagopal, 1980) was used (Orlov & Fortov, 2001) to carry out comparative analysis of the Thomas-Fermi model (TF) (Feynman *et al.*, 1949), the Hartree-Fock-Slater model (HFS) (Rozsnyai, 1972; Nikiforov & Uvarov, 1973), the Detail Configuration Accounting (DCA) (Rozsnyai, 1982), the Ion Model (IM) (Orlov, 1997), and a brief review of the models is available (Orlov, 2002). The general set of self-consistent field equations that describe the state of the whole ensemble of plasma atoms and ions has been obtained (Orlov & Fortov, 2001). The set contains (1) the Hartree-Fock equations for all atoms and ions with different electron configurations; (2) the unbound electron densities in phase space for all atoms and ions; (3) the Gibbs distribution; and (4) the electroneutrality condition. The main feature of this set is the general coupling of all equations for all plasma atoms and ions, including exited states. At first sight, the huge number of equations makes a solution of this set impossible. Therefore, further physical approximations were used, to simplify these equations until recently.

It should be noted that any simplification of the equations leads to a restricted range over which the model can be applied (Orlov & Fortov, 2001). For instance, the TF model can be used only for very high plasma temperatures, when practically all electrons are unbound. The well-known HFS model uses the average atom approximation, a fictitious atomic system with noninteger numbers of bound electrons in the atomic shells. These numbers are calculated using

https://doi.org/10.1017/S0263034610000777 Published online by Cambridge University Press

the Fermi-Dirac formula. Besides, the perturbation theory is used to calculate the properties of real atomic or ionic systems. If the temperature of the plasma decreases, this model cannot provide accurate enough results, and the limitation is connected with the application of perturbation theory. The DCA model uses the Hartree-Fock equations for real atomic and ionic systems and the Saha method for calculating their concentrations. This approach leads to an arduous problem for high-Z chemical elements (Rozsnyai, 1982). Moreover, it cannot be used for strongly coupled plasmas because of a peculiarity of the Saha method.

Thus, one can indicate the range of plasma temperatures and densities over which the TF, HFS, and DCA models cannot provide accurate enough results because the corresponding additional physical approximations are invalid. Of course, the mentioned ranges are different for different chemical elements (Orlov & Fortov, 2001). This fact makes it difficult to apply the TF, HFS, and DCA models to compound chemical compositions.

The solution of the general set of self-consistent field equations that describe the state of the whole ensemble of plasma atoms and ions is the way to solve the problem in general. The IM of hot dense plasma (Orlov, 1997) has been developed to achieve this aim. In a first step, the general set of equations was solved for "pure" substances, and then it was solved for compound chemical compositions (Orlov, 1987). As a result, reliable quantum mechanical calculations of radiative opacity became possible over a wide range of plasma densities and temperatures. The next step was connected with the optimization problem. A theoretical method and corresponding computer code were created to find out the optimal chemical composition of material that can be used as X-ray source material in practice, and the found material provides an optimal radiation yield (Orlov, 1999; Denisov *et al.*, 2005). The efficiencies of X-ray source materials can be estimated theoretically for both optically thick and optically thin plasma.

2.1. Optically Thick Plasma

Optically thick plasma can be produced by laser interaction with a hohlraum wall. It was shown (Orzechowski *et al.*, 1996) that hohlraum wall loss energy increases proportionally to the square root of the Rosseland mean free path l_R:

$$\Delta E \propto \left[l_R \tilde{\rho}\right]^{1/2}, \tag{1}$$

where $\tilde{\rho}(g/cm^3)$ is the plasma density. The radiation efficiency of hohlraum wall material increases with the reduction of the energy transported into the wall ΔE. It can be achieved by decreasing the Rosseland mean free path l_R. In this case, estimating the relative energy lost to the wall of two different materials α and β can be expressed as

$$\frac{\Delta E_\beta}{\Delta E_\alpha} = \left[\frac{l_R^\beta}{l_R^\alpha}\right]^{1/2}. \tag{2}$$

The value of ΔE (Eq. (1)) should be minimized to achieve the maximum hohlraum wall efficiency. Eq. (2) will be used below to estimate relative efficiency of different wall materials.

2.2. Optically Thin Plasma

Another approximation can be used for estimating the emissivity of optically thin plasma that can be produced by exploding wires. In this case, the outward energy flux increases inversely proportional to the Planck mean free path l_P :

$$j \propto \frac{1}{l_P}, \tag{3}$$

(Zeldovich & Raizer, 1966). The applicability range of the approximation was discussed by Orlov *et al.* (2007).

Eq. (3) can be used to estimate relative radiation efficiency of different exploding wires made of two different materials α and β:

$$k = \frac{j_\alpha}{j_\beta} = \frac{l_P^\beta}{l_P^\alpha}. \tag{4}$$

This approximate formula will be used below to compare theoretical and experimental results.

Thus, radiation efficiency increases with decreasing Rosseland or Planck mean free path for optically thick or optically thin plasma, respectively. Therefore, an optimal chemical composition for optically thick plasmas can be achieved by minimizing the Rosseland mean free path. In the case of optically thin plasmas, the Planck mean free path should be minimized.

The optimization problem was set up and settled by Orlov (1999), and more complete theoretical results were obtained by Denisov *et al.* (2005).

3. RESULTS OF CALCULATIONS AND EXPERIMENTAL DATA

3.1. Results of Calculations for Hohlraum Walls

As chemical admixtures can considerably influence the frequency-dependent opacity, and this fact can be used to improve the radiation efficiency of X-ray source materials, a simple 50/50 mixture of Au and gadolinium was proposed to reduce the radiation energy lost to the hohlraum walls in comparison with pure Au (Orzechowski *et al.*, 1996).

Table 1 presents Rosseland mean free paths l_R, which were calculated for different materials at the density $\tilde{\rho} = 1(g/cm^3)$ and different temperatures, using the IM of a plasma. Results are given for Au and for the composition (Au25.7%/W23.1%/Gd18.1%/Pr10.0%/Ba10.4%/Sb12.7%), which is denoted as Composition 1. Mass percentages of elements are given in the brackets. This composition was found

https://doi.org/10.1017/S0263034610000777 Published online by Cambridge University Press

Table 1. *Rosseland mean free path (cm) calculated for different materials at density* $\tilde{\rho} = 1(g/cm^3)$

T(eV)	Au	Comp. 1.	$\frac{l_R^{Au}}{l_R^{Comp1}}$	Au50/Gd50 (Comp.2)	$\frac{l_R^{Au}}{l_R^{Comp2}}$
150	3.21×10^{-4}	1.29×10^{-4}	2.49	2.47×10^{-4}	1.29
200	4.57×10^{-4}	1.53×10^{-4}	2.98	3.29×10^{-4}	1.39
250	5.01×10^{-4}	1.61×10^{-4}	3.11	2.89×10^{-4}	1.73
300	5.75×10^{-4}	1.87×10^{-4}	3.07	3.89×10^{-4}	1.48
350	6.35×10^{-4}	1.92×10^{-4}	3.31	4.37×10^{-4}	1.45

using an optimization method (Denisov *et al.*, 2005) that is more complete than that of Orlov (1999). Results are also presented for Composition 2 (Au50%/Gd50%) where, again, we have used mass fraction.

The spectral coefficients for X-ray absorption, $K(x)$ (cm^2/g), were calculated for different compositions at $T = 250$ eV and $\tilde{\rho} = 1\mathrm{g}/cm^3$ as functions of $x = \hbar\,\omega/T$. Figure 1 presents the coefficient calculated for Au (thick line). The coefficient is relatively small in the interval $(3.5 < x < 8.5)$ whereas the interval is overlapping with spectral lines for Composition 1 (thin line). It leads to decreasing Rosseland mean free path.

Table 2 presents the relative wall loss energy for different materials compared to a pure Au hohlraum wall as calculated by Suter *et al.* (1999), as well as some results of the present work, including Composition 1. Table 2 also presents the relative hohlraum wall loss energy for different materials as compared to AuGd hohlraum wall as calculated by Callahan-Miller and Tabak (2000). The result of the present work is also given (Composition 1). As shown, Composition 1 ensures higher radiation efficiency in comparison with other

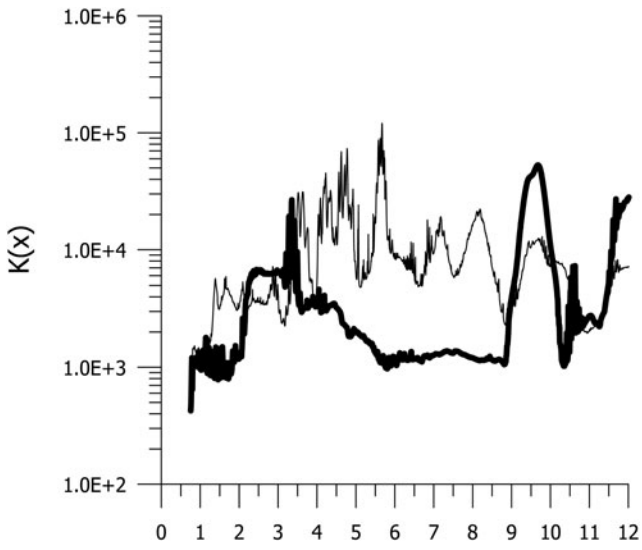

Fig. 1. The spectral coefficient of X-ray absorption $K(x)(\mathrm{cm}^2/\mathrm{g})$ calculated for Au (thick line) and for the Composition (Au25.7%/W23.1%/Gd18.1%/Pr10.0%/Ba10.4%/Sb12.7%) (thin line) at temperature $T = 250$ eV and density $\tilde{\rho} = 1\mathrm{g}/cm^3$.

Table 2. *The hohlraum wall loss energy for different materials, compared to a Au hohlraum wall* $\Delta\mathrm{E}_{wall}/\Delta\mathrm{E}_{Au}$ *and to a AuGd hohlraum wall* $\Delta\mathrm{E}_{wall}/\Delta\mathrm{E}_{AuGd}$

Au		AuGd	
Material	$\Delta E_{\mathrm{wall}}/\Delta E_{\mathrm{au}}$	Material	$\Delta E_{\mathrm{wall}}/\Delta E_{\mathrm{auGd}}$
Au	1.00	Au/Gd(50:50)	1.00
Au:Gd	0.83	Au	1.25
U:At:W:Gd:La	0.65	Pb	1.28
U:Bi:W:Gd:La	0.65	W	1.25
U:Bi:Ta:Dy:Nd	0.63	Pb/Ta(70:30)	1.06
Th:Bi:Ta:Sm:Cs	0.68	Hg/Xe(50:50)	1.18
U:Pb:Ta:Dy:Nd	0.63	Pb/Ta/Cs(45:20:35)	1.01
U:Nb.14:Au:Ta:Dy	0.66	Pb/Hf/Xe(45:20:35)	1.00
Comp. 1	0.57	Comp. 1	0.75

calculated compositions. Thus, the optimizing procedure (Denisov *et al.*, 2005), which can find out an effective complex material for a thick target, really can lead to better radiation efficiency materials.

3.2. Experimental and Theoretical Study of Exploding Wires in X-Pinch

The Rosseland and Planck mean free paths were also calculated for the NiCr alloy (Ni80%/Cr20%) and for Alloy 188 (Cr21.72%/Ni22.92%/Fe2.24%/Co39%/W13.93%) at temperature of $T = 1$ keV. Calculations were made at normal density $\tilde{\rho} = \tilde{\rho}_{normal}(g/cm^3)$, at density $\tilde{\rho} = 0.1^*\tilde{\rho}_{normal}(g/cm^3)$, and at density $\tilde{\rho} = 10^*\tilde{\rho}_{normal}(g/cm^3)$ (Tables 3 and 4). It was shown experimentally, that on the final stage of the X-pinch compression, the plasma density reaches values on the order of magnitude higher than the initial wire density. The most part of measured SXR is generated during this final stage, where plasma temperature and density reach maximum values (Orlov *et al.*, 2007).

Figure 2 presents the spectral coefficient for X-ray absorption $K(x)$ (cm^2/g) calculated for the NiCr alloy and Alloy 188 at temperature of $T = 1$ keV and density $\tilde{\rho} = 10^*\tilde{\rho}_{normal}(g/cm^3)$. The spectral coefficient for X-ray absorption of NiCr (thick line) is relatively small over the interval $(2.0 < x < 5.5)$ in comparison with the coefficient, which was calculated for Alloy 188 (thin line). This circumstance

Table 3. *Rosseland mean free path (cm) calculated for NiCr and Alloy 188 at temperature* T=*1 keV*

Density	l_R^{NiCr}	$l_R^{Alloy\ 188}$	$k = l_R^{NiCr}\ /\ l_R^{Alloy\ 188}$
$0.1^*\tilde{\rho}_{normal}$	2.54×10^{-1}	1.97×10^{-2}	12.89
$\tilde{\rho}_{normal}$	4.12×10^{-3}	1.37×10^{-3}	3.01
$10.^*\tilde{\rho}_{normal}$	1.11×10^{-4}	5.81×10^{-5}	1.91

https://doi.org/10.1017/S0263034610000777 Published online by Cambridge University Press

Table 4. *Planck mean free path (cm) calculated for NiCr and Alloy 188 at temperature* T=*1 keV*

Density	l_P^{NiCr}	$l_P^{Alloy\ 188}$	$k = l_P^{NiCr}/l_P^{Alloy\ 188}$
$0.1^*\tilde{\rho}_{normal}$	1.16×10^{-2}	2.83×10^{-3}	4.06
$\tilde{\rho}_{normal}$	2.99×10^{-4}	2.16×10^{-4}	1.38
$10.^*\tilde{\rho}_{normal}$	3.29×10^{-5}	1.78×10^{-5}	1.84

Table 5. *Theoretical and experimental results on the relative radiation energy yield from exploding wires made of NiCr and Alloy188*

	EXPERIMENT		THEORY	
Energy band	k ^{exper}	Δ^{exper}	k ^{theory}	Δ^{theory}
E > 1.5 keV	1.736	20%	1.84	5.6%
2.5< E < 5 keV	1.9	20%	1.84	3.2%

provides decreasing Rosseland and Planck mean free paths for Alloy 188 in comparison with NiCr and, therefore, improves the radiation efficiency of the corresponding wire.

Experimental measurements were carried out to study the radiative efficiency of substances and to test the theoretical results (Orlov *et al.*, 2007). The total energy yield B was measured using two devices with different spectral bands. The experimental coefficient of relative efficiency can be expressed in the form

$$k^{\text{exper}} = B^{\text{Alloy188}}/B^{\text{NiCr}}. \tag{5}$$

The theoretical coefficient of relative efficiency has the form

$$k^{\text{theor}} = j^{\text{Alloy188}}/j^{\text{NiCr}} = l_P^{NiCr}/l_P^{Alloy188}, \tag{6}$$

in accordance with Eq. (4). Table 5 compares theoretical and experimental results concerning relative efficiency of exploding wires made of Alloy 188 and NiCr (Orlov *et al.*, 2007). Here Δ^{exper} is the experimental error band, Δ^{theory} is deviation of theoretical results from experimental data. As shown, theoretical results agree well with the experimental data. Thus, experimental study confirmed the theoretical results.

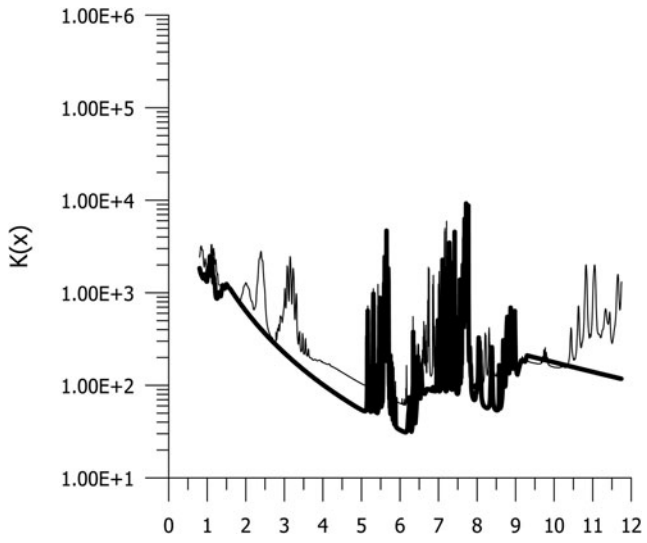

Fig. 2. The spectral coefficient of X-ray absorption $K(x)(\text{cm}^2/\text{g})$ calculated for NiCr (thick line) and for the composition Alloy 188 (Cr21.72%/Ni22.92%/Fe2.24%/Co39%/W13.93%) (thin line) at temperature $T = 1$ keV and density $\tilde{\rho} = 10^*\tilde{\rho}_{normal}$.

3.3. Symmetric Multilayer X-Pinch Study

Previously studied cases were connected with big differences between the Rosseland or Planck mean free paths for different substances. A more complicated case is connected with the so-called symmetric multilayer X-pinch, where tungsten W and molybdenum Mo wires have been used (Shelkovenko *et al.*, 2010). The structure of multilayer X-pinch plasma is given in Figure 3. The structure provides higher radiation efficiency than pure tungsten (Table 6). Table 6 presents radiation powers generated in experiments with a symmetric multilayer X-pinch within different energy bands (Shelkovenko *et al.*, 2010). The experimental coefficient of relative efficiency can be expressed here in the form

$$k^{\text{exper}} = P^{\text{WMo}}/P^{\text{W}}. \tag{7}$$

The theoretical explanation is connected with specific spectral coefficients for X-ray absorption and radiation. Figure 4 presents the spectral coefficient for X-ray absorption K(E) (cm^2/g) calculated for W and the spectral coefficient for X-ray radiation $J(E)$ (a.u.) calculated for Mo at plasma temperature of $T = 1$ keV and the densities, which are 10-times higher than the initial solid wire densities. One can see that the energy interval of maximal radiation for Mo coincides

Fig. 3. The structure of a multilayer X-pinch plasma, where tungsten and molybdenum wires are used.

https://doi.org/10.1017/S0263034610000777 Published online by Cambridge University Press

Table 6. *Radiation powers generated in experiments with a symmetric multilayer X-pinch within different energy bands*

X-pinch composition	Radiation power P(GW) $E>1.5$ keV	Radiation power P(GW) $2.5 < E < 5$ keV
W	1.3 ± 0.2	0.4 ± 0.03
W, Mo	2.7 ± 0.3	1.2 ± 0.06
k^{exper}	2.08	3.0

Table 7. *Rosseland and Planck mean free paths (cm) calculated for W and mixture (W80%, Mo20%) at* T=*1 keV and density* $\tilde{\rho} = 10^{*}\tilde{\rho}_{norm}$

Substances	l_R	l_P
W	1.26×10^{-5}	1.64×10^{-6}
mixture W80%, Mo20%	1.49×10^{-5}	1.79×10^{-6}

with the interval of maximal absorption for W. Therefore, practically all radiation of Mo is absorbed in W. The effect leads to additional heating or preheating of the W plasma. One can note that 20% of additional temperature provides double increasing of radiation power.

A very important question is connected with possible intermixing of components of structure under high compression (Fig. 3). To answer this question, the Rosseland and Planck mean free paths were calculated at $T = 1$ keV and density $\tilde{\rho} = 10^{*}\tilde{\rho}_{norm}$ for W and for the mixture (W80%/Mo20%). The results are given in Table 7. In accordance with these results, the Planck mean free path for the mixture (W80%/Mo20%) exceeds the Planck mean for W, and the theoretical coefficient of relative efficiency (4) has the value $k^{\text{theor}} = j^{\text{WMo}}/j^{\text{W}} = 0.92$. On the other hand, the experimental coefficient of relative efficiency equals $k^{\text{exper}} = M^{\text{WMo}}/M^{\text{W}} = 2.08$ for photon energies up $E > 1.5$ keV and $k^{\text{exper}} = M^{\text{WMo}}/M^{\text{W}} = 3.0$ for a photon range 2.5 keV $< E < 5$ keV (Table 6). Thus, intermixing of components leads to the decreasing radiative efficiency in the considered case, and it contradicts the experimental results. One can conclude that component intermixing is absent. Additional experimental facts confirm this conclusion. Indeed, spectral lines of MO have not been measured experimentally, what would not be the case would components undergo intermixing (Shelkovenko *et al.*, 2010). Thus, based on experimental and theoretical results, one can assert that component intermixing is absent in symmetric multilayer X-pinch.

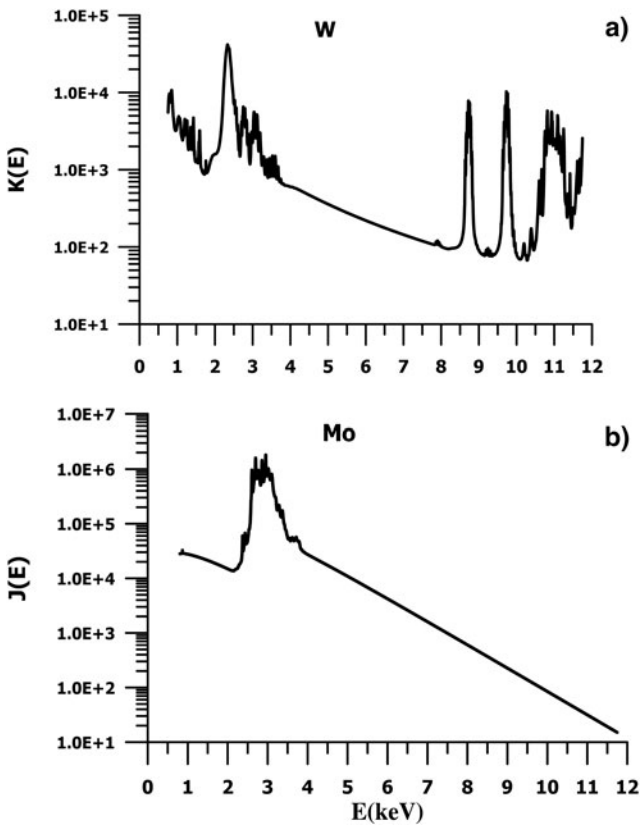

Fig. 4. The spectral coefficient for X-ray absorption $K(E)$ (cm^2/g) calculated for W and the spectral coefficient for X-ray radiation $J(E)$ (a.u.) calculated for Mo at plasma temperature $T = 1$ keV and density $\tilde{\rho} = 10^{*}\tilde{\rho}_{norm}$.

3.3.1. Application of the Ion Model of Plasma for Theoretical and Experimental Study of Plasma Targets Obtained Via Indirect Heating of Low-Z Foams

In this section, the IM of plasma was used in order to describe the radiative properties of indirectly heated low-Z foams used in the experimental study of heavy ion energy loss in laser produced plasma. When the heavy ion beam propagates in ionized matter one expects increased ion energy loss compared to the interaction with "cold" target caused by two important effects: more effective energy transfer from projectile ions to free plasma electrons compared to the transfer to the bound electrons; and due to increased projectile charge state in ionized matter caused by the suppression of the target bound electron capture process. For the first time these effects were demonstrated in low density low temperature Hydrogen gas-discharge (Hoffmann *et al.*, 1990; Jacoby *et al.*, 1995). Using the laser produced plasma targets one can expand the region of plasma parameters and investigate the ion stopping process at higher plasma temperatures and densities. For the correct interpretation of experimental results on the ion energy loss in ionized matter, the knowledge of plasma target parameters existing over the time of heavy ion beam-plasma interaction is of great importance.

3.3.2. Experimental Study of Plasma Targets Obtained By Indirect Heating of Low Density Polymer Foams

In experiments on the interaction of heavy ions with ionized matter, a high density plasma target with homogeneous

https://doi.org/10.1017/S0263034610000777 Published online by Cambridge University Press

in time (~5 ns) and space (~1 mm) plasma parameters is required. The time is defined by the duration of the heavy ion micro-bunch of 3 ns, the spatial size of the plasma target by the diameter of the heavy ion beam of ~0.5 mm. The experimental accuracy of synchronization the heavy ion beam and laser pulses is of 1 ns. Highly homogeneous and slow expended plasma targets can be obtained when polymer low density foams are volumetrically heated by means of soft X-rays. Low-Z plasma target is required in order to increase the ratio of free-to-bound electrons in plasma target and to make a plasma effect on the heavy ion energy loss more pronounced.

The indirect laser target design was proposed for combined heavy ion-laser experiments by Vasina and Vatulin (2000). In this scheme, the laser interacts with the wall of the Au cylindrical converter (primer hohlraum) where effective conversion of the laser energy into the soft X-rays having a close to the Planck spectral distribution takes place. Generated hohlraum X-ray radiation heats volumetrically the low-density foam which serves as a plasma target for probing with heavy ion beams. Figure 5 shows the geometry of the laser-target interaction.

Foam materials (Khalenkov *et al.*, 2006) are very promising for these purposes due to the effective conversion of the deposited radiation energy into the internal plasma energy and slow hydrodynamic response on heating. Direct irradiation of the Au converter walls with a ns laser pulse leads to soft X-ray hohlraum spectra caused by O-shell transitions in Au. Expected temperatures of the foam targets heated by this radiation amount to 20–30 eV at electron densities of 10^{21} cm^{-3}.

In experiments (Rosmej *et al.*, 2009), the combined targets which consisted on the cylindrical primer hohlraum (converter) of 1.5–1.7 mm in diameter and a foam/foil target placed from the rear convertor side were used. Thin Au foil of 100 nm thickness placed between converter and foam target prevented direct irradiation of foams with the laser light.

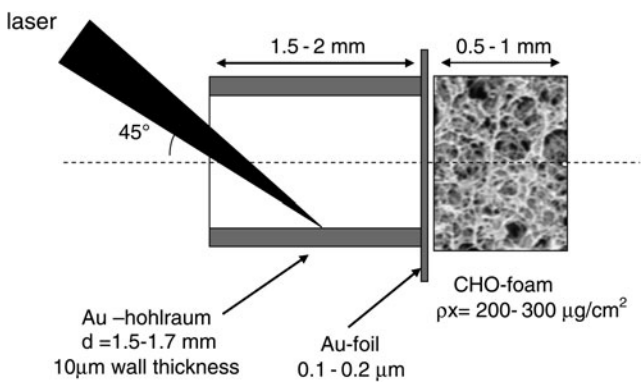

Fig. 5. Geometry of the laser pulse interaction with the combined target, which consists of the primary hohlraum (converter), thin Au foil and foam or foil target placed on the rear side.

A variety of foam/foil materials such as Agar-Agar ($C_6H_{10}O_5$), Plexiglas (PMMA, $C_8H_8O_3$), and triacetate cellulose (TAC, $C_{12}H_{16}O_8$) of different volumetric and area densities were used. The pore size varies from 10–50 μm for agar-agar down to 1 μm for TAC. The small pore size of foam targets is of big importance both for laser and heavy ion beam interaction preventing the broadening heavy ion energy spectra when an ion beam penetrates a cold porous target and keeping the plasma homogenization time after irradiation by laser/soft X-rays in sub-ns range.

The Petawatt High-Energy Laser System for Ion beam Experiments (PHELIX) (Nd:glass, $\lambda = 1053$ nm) was used at the basic frequency (Bagnoud *et al.*, 2010). The laser pulse of 1.4 ns duration and energies up to 150 J was focused onto the target by a lens with 4 m focal length. The diameter of the focal spot on the wall of the primer hohlraum was of 300–400 μm, resulting in laser intensities of up to 2×10^{14} W/cm^2. The laser with an incidence angle of 45° irradiates the wall of the Au cylinder through the open entrance hole (see Fig. 5). The time depended behavior of the hohlraum radiation was measured, using soft X-ray diodes with Carbon cathode. The diode system allows absolute measurements in the photon energy region of 300–1000 eV. The typical duration of the X-ray signal was about 5–7 ns. The spectrally resolved hohlraum radiation in the photon energy range of 1–20 nm was analyzed by means of an absolute calibrated slit grating spectrograph based on an e-beam written 10,000 line-pairs/mm free-standing transmission diffraction grating (Wilhein *et al.*, 1999). In combination with a thinned, back-illuminated charge coupled device (CCD), the spectrograph can be used for real-time spectroscopy of laser-produced plasma X-ray sources. Calibration of the grating and CCD allows absolute photon flux measurements. The transmitted grating spectrometer (TGS) was used in experiments without entrance slit in order to increase the photon flux and to improve the signal-to-noise ratio. The spectral resolution $\Delta\lambda$ was between 0.1 and 0.2 nm depending on the source size (1–2 mm) and the observation range (1–6 nm or 1–20 nm). The spectrometer system including CCD was calibrated at DESY. In experiments, spectral distribution of the hohlraum radiation field from the target rear side was measured. For these purposes, convertor targets (primer hohlraums) without foam/foil were used. As the next step hohlraum spectra transmitted through the foam/foil placed at the rear side of the combined target were measured (Rosmej *et al.*, 2010). Due to effective absorption of soft X-rays in foam/foils, targets were heated to plasma. Figure 6 (color online) shows the spectra irradiated by the Au hohlraum plasma and recorded after transmission through the "cold" 0.5 μm thick Carbon filter (green) placed at the TGS-entrance for calibration purposes and 0.5 μm thick CHO-foil (red) indirect heated with 130 J PHELIX-laser pulse of 1.4 ns duration. In the case of the "cold" C-filter, one can see the sharp absorption K-edge at 4.2–4.4 nm wave length. The step-like form of the

https://doi.org/10.1017/S0263034610000777 Published online by Cambridge University Press

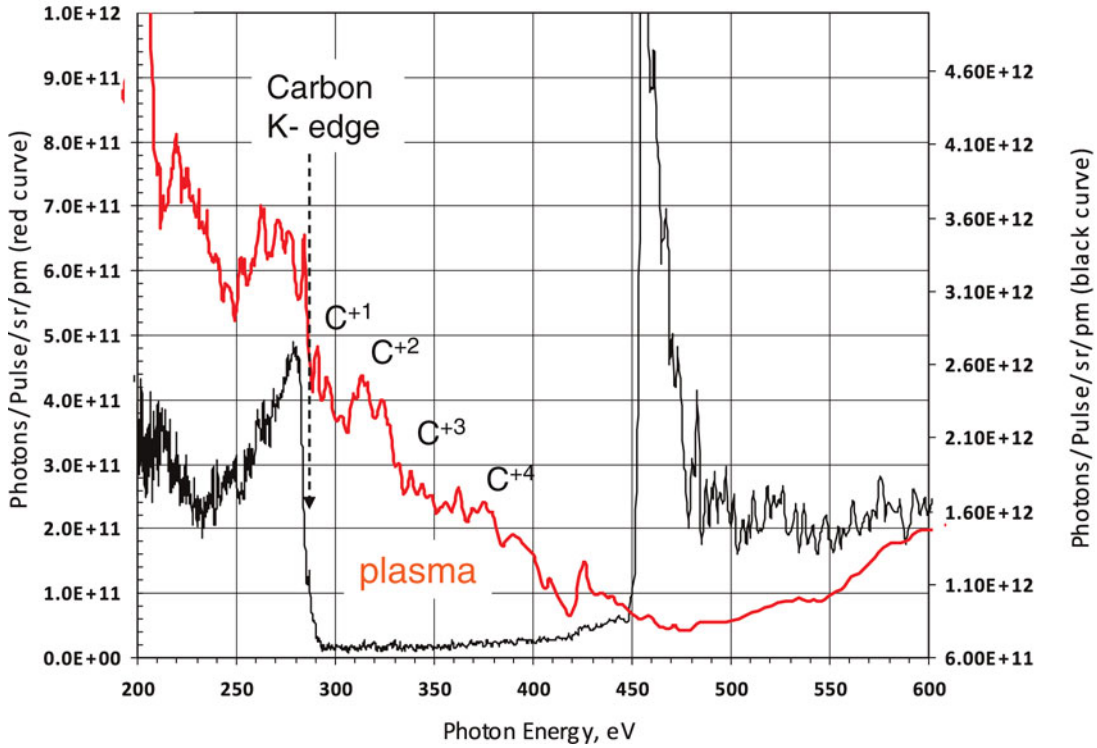

Fig. 6. (Color online) Comparison of the absolute calibrated hohlraum spectra transmitted through the indirectly heated CHO-foil at 130 J laser energy (red curve) and the 0.5 μm thick "cold" Carbon filter (red curve) placed at the TGS-entrance for calibration purposes. CHO-foil was of a 0.5 μm thickness and 1.1 g/cm^3 initial density, a corresponding area density is of 55 μg/cm^2.

deformed Carbon K-edge (red) occurs in plasma and can be attributed to the presence of the ionized carbon atoms with charges up to Z = 4. The He-like Carbon ion (+4) fraction calculated by means of a radiative-collisional code FLYCHK (Chang *et al.*, 2005) for plasma with electron density of 10^{21} cm^{-3}, 800 μm thickness and temperatures from 5 up to 20 eV, does not exceed 5% at plasma temperature of 10 eV and is significantly present in the plasma at T_e = 15–20 eV. Therefore, the experimental results allow supposing an electron temperature of the CHO-foil heated by soft X-rays higher than 10 eV.

Figure 7 demonstrates experimental results on the indirect heating of a 500 μm thick CHO-foam of 10 mg/cm^3 mean density. It can be obviously seen that the target with 10 times higher area density than the CHO-foil couldn't be homogeneous heated with 70 J laser pulse. The K-edge deformation due to the plasma effect like in the previous figure is absent; the foam target (red curve) transmits radiation as a "cold" filter (black curve) with a sharp K-edge position at 4.2–4.4 nm (285–290 eV).

A method which applies the deformation of the Carbon absorption K-edge when cold matter is heated to plasma is now under development. There are at least two reasons why traditional diagnostic methods using plasma self radiation is not applicable in this case. First, the most intensive radiation of Carbon plasma at expected temperatures of 10–30 eV occurs due to L-shell transition, containing a lot of lines broad due to the high optical thickness of the plasma target and form a quasi-continuum; second: the energy range of hohlraum radiation (O-shell transition of Au) overlaps with the L- shell transitions in Carbon and has in our case an order of magnitude higher photon flux.

The dependence of the absorption K-edge position on the energy scale on the plasma ionization degree seems to be a promising diagnostic instrument. In cold Carbon, increased photo-absorption occurs when the photon energies approach the binding energy of the K-shell electrons in the C-atom. For cold Carbon, the K-edge position corresponds to 285 eV photon energy. In plasma, the Carbon outer-shell electrons will be ionized in collisions with free plasma electrons and the target ionization degree depends mostly on the plasma electron temperature. Due to lower screening potentials of outer-shell electrons in ionized atoms, the K-shell electron binding energy and as a consequence the positions of the K-edges for the subsequent charge states will be shifted to the higher photon energies. According to Dirac-Fock-Slater calculations (Zschornack *et al.*, 1986) for isolated Carbon ions, one obtains the following K-edge energies for different Carbon charge states: C^{+1} = 297.7 eV; C^{+2} = 313, 39 eV; C^{+3}= 346.17 eV; C^{+4}= 380.51 eV. In plasmas compared to cold matter, calculations of the K-edge positions and plasma opacities are complicated since one has to take into

https://doi.org/10.1017/S0263034610000777 Published online by Cambridge University Press

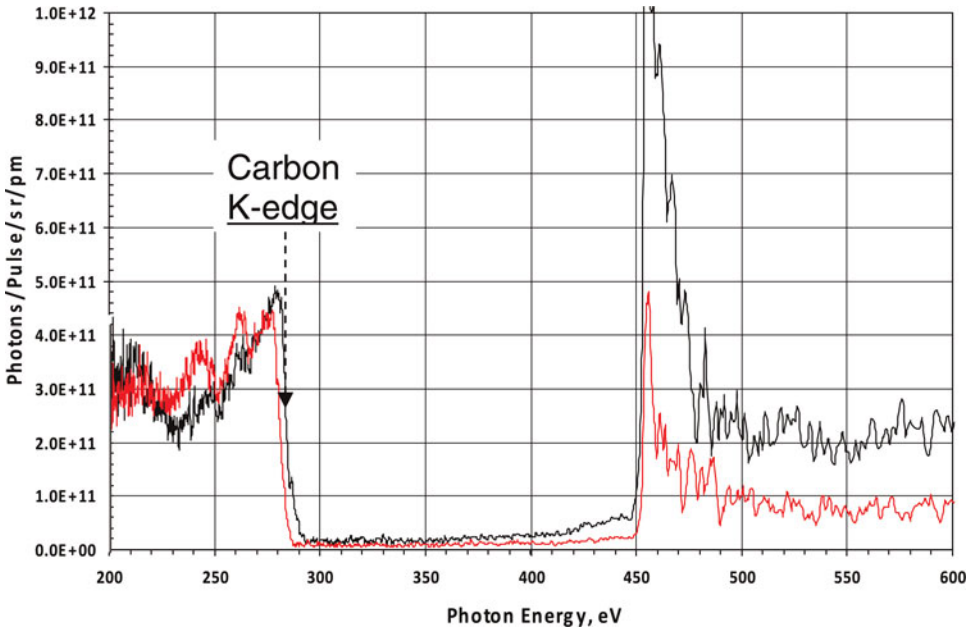

Fig. 7. (Color online) Comparison of the absolutely calibrated hohlraum spectra transmitted through the indirectly heated CHO-foam (red curve) and the 0.5 μm thick "cold" Carbon filter (red curve) at laser energy of 70 J; CHO-foam is of 10 mg/cc density and 500 μm thickness corresponding to 500 μg/cm^2 area density.

account many new factors: a charge state distribution of the ions, the population of ion states excited in collisions with free plasma electrons, effects of plasma microfields etc. in dependence on plasma parameters.

The theoretical approach, which was used in previous items of this paper, gives, in particular, K-edge energies of different plasma ions in ground and excited states, and provides calculations of the spectral coefficients for X-ray absorption as well as the spectral characteristics of radiation transmitted through the CHO plasma target depending on plasma parameters. Comparison of the theoretical and experimental results can be used to estimate the plasma temperature and ionization degree. The quantitative interpretation of the time-integrated spectrum shown in Figure 6 is hardly possible due to fast hydrodynamic expansion of the heated foil where the target density drops many times in subnanosecond time scale. One-dimensional calculations of the hydrodynamic expansion of a 2–3 mg/cc 1000 μm thick CHO-foam heated up to 10–30 eV demonstrate promising stability of the plasma temperature and density profiles during first 8–10 ns (Vergunova *et al.*, 2010). In future experiments, we are going to measure the hohlraum radiation field without and with foam target placed on the converter rear-side and then compare results with calculated theoretical spectra in dependence on plasma temperature.

3.3.3. Theoretical Justification for the Temperature Diagnostic of Indirectly Heated Low Density Foams

The theoretical approach that was developed and used in previous studies can be applied in order to give a theoretical justification for a temperature diagnostic of low density polymer foams heated by means of SXR. The IM allows, in particular, calculating K-edge energies of different plasma ions in ground, and excited states and the spectral coefficients for X-ray absorption as well as the spectral characteristics of radiation transmitted through the CHO-plasma target. For the interpretation of experimental results on opacities of the indirectly heated TAC-foams, calculations of absorption coefficient of $H_{12}C_8O_6$ plasma at initial foam mean density of 2 mg/cm^3 and for different plasma temperatures were carried out. According to hydrodynamic simulations on the foam heating by soft X-rays, the constant plasma density is guaranteed over 10 ns after the beginning of the heating pulse for foam thickness of 800 μm (Vergunova *et al.*, 2010). This foam feature is of big importance for interpretation of obtained experimental results.

Besides the absorption coefficients, the Planck spectra with radiative temperature of 40 eV transmitted through the plasma target is calculated. These theoretical results can be compared with the spectra measured from the rear target side by means of TGS spectrometer. Figure 8a shows the spectral coefficients for X-ray absorption K (E) (cm^2/g) calculated for ($H_{12}C_8O_6$) plasma at density 0.002 (g/cc) and temperature $T = 5$ eV. The K-edge positions of carbon ions are denoted here with corresponding notations, which present the electron configurations 1s(2)2s(2)2p(1) and 1s(2)2s(1)2p(1). Figure 8b also presents the spectral characteristics of Planck radiation J(E) (J/keV/sr/cm^2) transmitted through the CHO plasma target with 5 eV temperature and the initial mean density. Function J(E)

https://doi.org/10.1017/S0263034610000777 Published online by Cambridge University Press

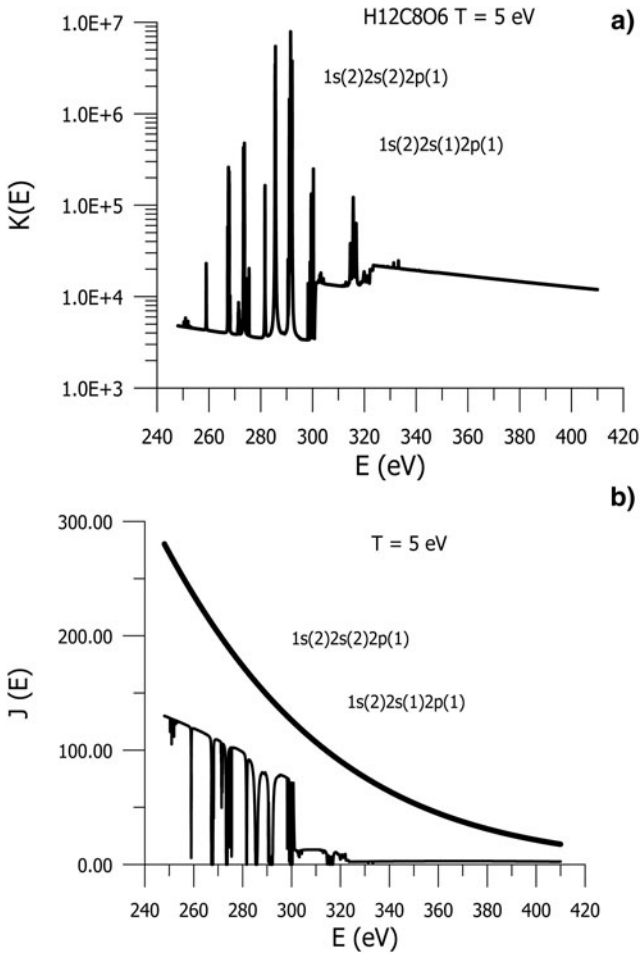

Fig. 8. The spectral coefficients for X-ray absorption $K(E)$ (cm^2/g) (**a**) calculated for ($H_{12}C_8O_6$) plasma at the density 0.002 (g/cc) and temperature $T = 5$ eV and the spectral characteristic of radiation $J(E)$ ($J/keV/sr/cm^2$) (**b**) transmitted through the ($H_{12}C_8O_6$) plasma target. The super bold line on the picture (b) gives the spectrum of the external radiation.

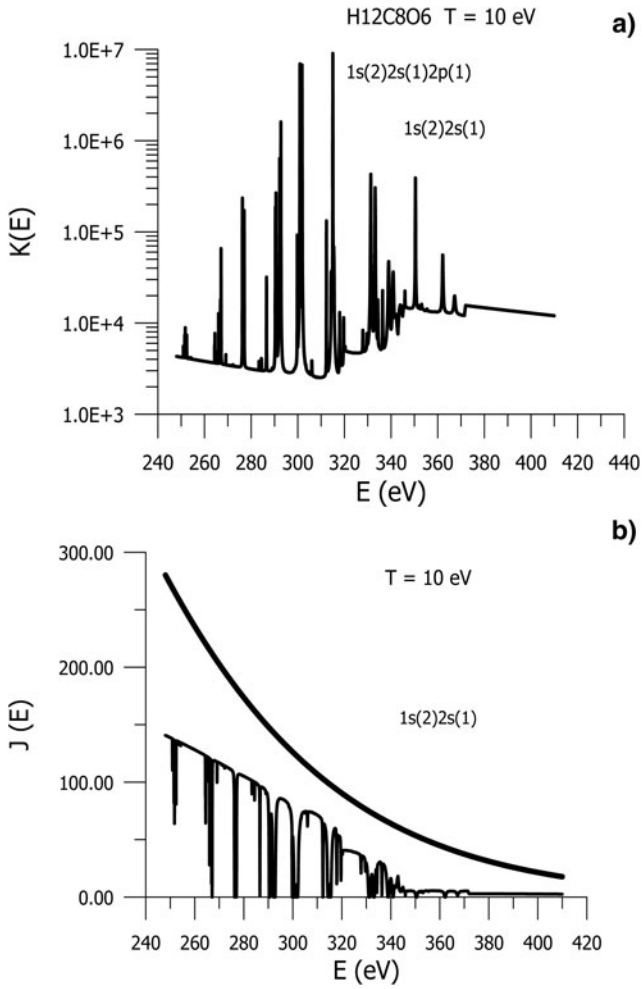

Fig. 9. The spectral coefficients for X-ray absorption $K(E)$ (cm^2/g) (**a**) calculated for ($H_{12}C_8O_6$) plasma at the density 0.002 (g/cc) and temperature $T = 10$ eV and the spectral characteristics of radiation $J(E)$ ($J/keV/sr/cm^2$) (**b**) transmitted through the ($H_{12}C_8O_6$) plasma target. The super bold line on the picture (b) gives the spectrum of the external radiation.

represents the spectral intensity of transmitted radiation multiplied by the duration of the X-ray radiation of 5 ns. The super bold line gives the spectrum of external radiation, which was approximated with Planck function at radiation temperature $T_{rad} = 40$ eV. One can see that the K-edge position of carbon ion 1s(2)2s(2)2p(1) (Fig. 8a) coincides with the specific step of spectral characteristics of transmitted radiation J(E) (Fig. 8b) on the energy scale. Similar calculations were made for the temperature $T = 10$ eV. (Fig. 9) and $T = 20$ eV (Fig. 10). The specific step of the function $J(E)$ (Fig. 9b) coincides with the K-edge position of carbon ion 1s(2)2s(1) (Fig. 9a), and the step of $J(E)$ (Fig. 10b) coincides with the K-edge position of carbon ion 1s(2) (Fig. 10a).

Comparison of the theoretical functions $K(E)$ and $J(E)$ with measured experimentally can be used to estimate temperature and ionization degree of indirectly heated foam targets.

4. CONCLUSIONS

We have shown that the theoretical method presented in this paper provides reasonable results on estimating the radiation efficiency of the materials heated by pulsed current devises or lasers and used as X-ray sources. This method can be used in order to determine effective complex materials for exploding wires, thick laser targets, hohlraums etc. in dependence on plasma density and temperature. The theoretical approach can also be applied to the analysis of physical effects that were obtained in experiments with a symmetric multilayer X-pinch. Finally, the theoretical method was used for calculations of absorption coefficients of low density CHO-foams heated volumetrically by soft X-rays. The method for the diagnostics of plasma temperature reached in foam-layers is proposed, based on the experimentally observed deformation of the absorption K-edge when foam is heated to plasma.

https://doi.org/10.1017/S0263034610000777 Published online by Cambridge University Press

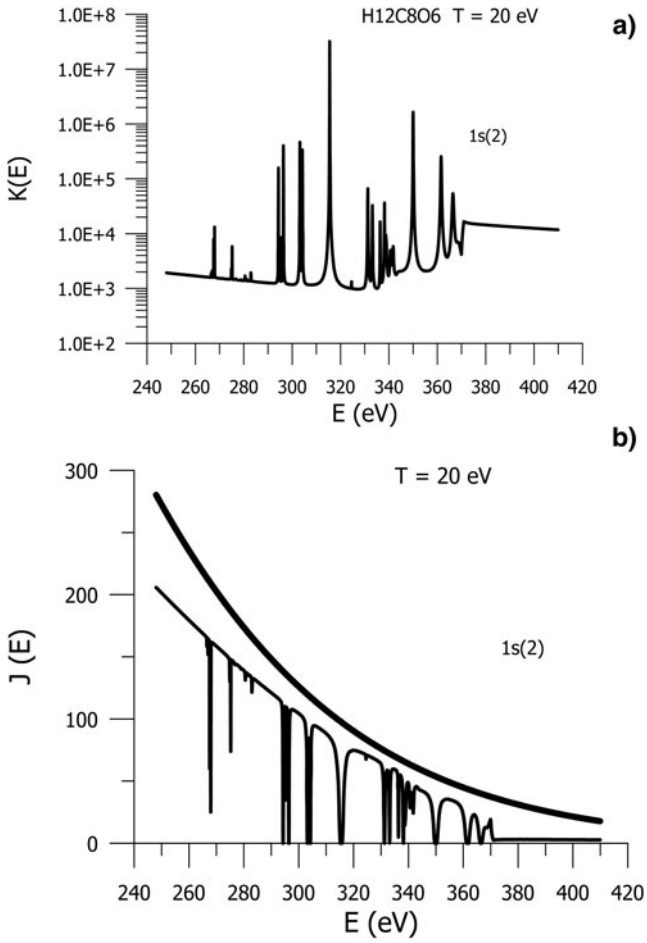

Fig. 10. The spectral coefficients for X-ray absorption $K(E)$ (cm^2/g) (**a**) calculated for $(H_{12}C_8O_6)$ plasma at density 0.002 (g/cc) and temperature $T = 20$ eV and the spectral characteristics of radiation $J(E)$ $(J/keV/sr/cm^2)$ (**b**) transmitted through the $(H_{12}C_8O_6)$ plasma target. The super bold line on the picture (b) gives the spectrum of the external radiation.

REFERENCES

Adamek, P., Renner, O., Drska, L., Rosmej, F.B. & Wyart, J.F. (2006). Genetic algorithms in spectroscopic diagnostics of hot dense plasmas. *Laser Part. Beams* **24**, 511–518.

Bagnoud, V., Aurand, B., Blazevic, A., Borneis, S., Bruske, C., Ecker, B., Eisenbarth, U., Fils, J., Frank, A., Gaul, E., Goette, S., Haefner, C., Hahn, H., Harres, K., Heuck, H.-M., Hochhaus, D., Hoffmann, D.H.H., Javorková, D., Kluge, H.-J., Kuehl, T., Kunzer, S., Kreutz, M., Merz-Mantwill, T., Neumayer, P.,Onkels, E., Reemts, D., Rosmej, O., Roth, M., Stoehlker, T., Tauschwitz, A., Zielbauer, B., Zimmer, D. & Witte, K. (2010). Commissioning and early experiments of the PHELIX facility. *Appl. Phys. B* **100**, 137–150.

Batani, D., Dezulian, R., Redaelli, R., Benocci, R., Stabile, H., Canova, F., Desai, T., Lucchini, G., Krousky, E., Masek, K., Pfeifer, M., Skala, J., Dudzak, R., Rus, B., Ullschmied, J., Malka, V., Faure, J., Koenig, M., Limpouch, J., Nazarov, W., Pepler, D., Nagai, K., Norimatsu, T. & Nishimura, H. (2007). Recent experiments on the hydrodynamics of laser-produced plasmas conducted at the PALS laboratory. *Laser Part. Beams* **25**, 127–141.

Borisenko, N.G., Akunets, A.A., Bushuev, V.S., Dorogotovtsev, V.M. & Merkuliev, Y.A. (2003). Motivation and fabrication methods for inertial confinement fusion and inertial fusion energy targets. *Laser Part. Beams* **21**, 505–509.

Bret, A. & Deutsch, C. (2006). Density gradient effects on beam plasma linear instabilities for fast ignition scenario. *Laser Part. Beams* **24**, 269–273.

Callahan-Miller, D. & Tabak, M. (2000). Progress in target physics and design for heavy ion fusion. *Phys. Plasmas* **7**, 2083–2091.

Chang, H.-K., Chen, M.H., Morgan, W.L., Ralchenko, Y. & Lee, R.W. (2005). FLYCHK: Generalized population kinetics and spectral model for rapid spectroscopic analysis for all elements. *Hi. Energy Density Phys*. **1**, 3–12.

Denisov, O.B., Orlov, N.Yu., Gus'kov, S.Yu., Rozanov, V.B., Zmitrenkop, N.V. & Michailov, A.P. (2005). Modelling of the composition of materials for soft X-ray sources used in research on inertial confinement fusion. *Plasma Phys. Rept*. **31**, 684–689.

Feynman, R., Metropolis, N. & Teller, E. (1949). Equations of state of elements based on the generalized Fermi-Thomas theory. *Phys. Rev*. **75**, 73–79.

Gus'kov, S.Y. (2005). Thermonuclear gain and parameters of fast ignition ICF-targets. *Laser Part. Beams* **23**, 255–260.

Hoffmann, D.H.H., Blazevic, A., Ni, P., Rosmej, O., Roth, M., Tahir, N.A., Tauschwitz, A., Udrea, S., Varentsov, D., Weyrich, K. & Maron, Y. (2005). Present and future perspectives for high energy density physics with intense heavy ion and laser beams. *Laser Part. Beams* **23**, 47–53.

Hoffmann, D.H.H., Weyrich, K., Wahl, H., Gardes, D., Bimbot, R. & Fleurier, C. (1990). Energy loss of heavy ions in a plasma target. *Phys. Rev. A*, **42**, 2313–2321

Hora, H. (2007). New aspects for fusion energy using inertial confinement. *Laser Part. Beams* **25**, 37–45.

Jacoby, J., Hoffmann, D.H.H., Laux, W., Mueller, R.W., Wahl, H., Weyrich, K., Boggasch, E., Heimrich, B., Stoeckl, C. & Wetzler, H. (1995). Stopping of heavy ions in a Hydrogen plasma. *Phys. Rev. Lett*. **74**, 1550–1553.

Khalenkov, A.M., Borisenko, N.G., Kondrashov, V.N., Merkuliev, Yu.A., Limpouch, J. & Pimenov, V.G. (2006). Experience of micro-heterogeneous target fabrication to study energy transport in plasma near critical density. *Laser Part. Beams*. **24**, 283–290.

Kilkenny, J.D., Alexander, N.B., Nikroo, A., Steinman, D.A., Nobile, A., Bernat, T., Cook, R., Letts, S., Takagi, M. & Harding, D. (2005). Laser targets compensate for limitations in inertial confinement fusion drivers. *Laser Part. Beams* **23**, 475–482.

Koresheva, E.R., Osipov, I.E. & Aleksandrova, I.V. (2005). Free standing target technologies for inertial fusion energy: Target fabrication, characterization, and delivery. *Laser Part. Beams* **23**, 563–571.

Kyrala, G.A., Delamater, N., Wilson, D., Guzik, J., Haynes, D., Gunderson, M., Klare, K., Watt, R.W., Wood, W.M. & Varnum, W. (2005). Direct drive double shell target implosion hydrodynamics on OMEGA. *Laser Part. Beams* **23**, 187–192.

Lindl, J.D. (1998). Inertial Confinement Fusion, AIP Press, Springer, New York

March, N.H., Kohn, W., Vashishta, P., Lundquist, S., Williams, A.R., Lang, N.D. & Von Barth, U. (1983). *Theory of the Inhomogeneous Electron Gas*. New York: Plenum Press.

https://doi.org/10.1017/S0263034610000777 Published online by Cambridge University Press

Ng, A., Ao, T., Perrot, F., Dharma-Wardana, M.W.C. & Foord, M.E. (2005). Idealized slab plasma approach for the study of warm dense matter. *Laser Part. Beams* **23**, 527–537.

Nikiforov, A. & Uvarov, V. (1973). Opisanie sostoyaniya veschestva v oblasti visokoch temperatur na osnove uravnenii samosoglasovannogo polya (Description of a substunce state at high temperatures based on the self-consistent field equations). *Chislennye metodi mech. sploscnoi sredi*. **4**, 114–117. (in Russian).

Orlov, N.Yu. (1987). Quantum statistical calculations of the properties of a mixture of chemical elements allowing for fluctuations in the occupation numbers of electron states. *USSR Comput. Math. Mathem. Phys*. **27**, 64–70.

Orlov, N.Yu. (1997). Ion model of a hot dense plasma. *Laser and Part. Beams* **15**, 627–634.

Orlov, N.Yu. (1999). Calculation of the radiative opacity of a hot dense plasma. *Contrib. Plasma Phys*. **39**, 177–180.

Orlov, N.Yu. (2002). Theoretical models of hot dense plasmas for inertial confinement fusion. *Laser Part. Beams* **20**, 547–549.

Orlov, N.Yu. & Fortov, V.E. (2001). Comparative analysis of the theoretical models of a hot dense plasma and the density functional theory. *Plasma Phys. Rept*. **27**, 44–55.

Orlov, N.Yu., Guśkov, S.Yu., Pikuz, S.A., Rozanov, V.B., Shelkovenko, T.A., Zmitrenko, N.V. & Hammer, D.A. (2007). Theoretical and experimental studies of the rsdiative properties of hot dense matter for optimizing soft X-ray sources. *Laser Part. Beams* **25**, 1–9.

Orzechowski, T.J., Rosen, M.D., Korblum, M.D., Porter J.L., Suter, L.J., Thissen, A.R. & Wallace, R.J. (1996). The Rosseland Mean Opacity of a Mixture of Gold and Gadolinium at High Temperatures. *Phys. Rev. Lett*. **77**, 3545–3548.

Rajagopal, A.K. (1980). Theory of inhomogeneous electron systems: spin-density-functional formalism. *Advan. Chem. Phys*. **41**, 59–193.

Rosmej, O.N., Orlov, N., Schäfer, D., Nisius, T., Wilhein, T., Suslov, N., Zhidkov, N. & Zhao, Y. (2009). Diagnostics of temperature and ionization degree of low Z foams in experiments on the ion stopping in plasma. *GSI Scientific Report 2009*, 391.

Rosmej, O.N., Zhidkov, N., Vatulin, V., Sulov, N., Kunin, A., Nisius, T., Zhao, Y., Wilhein, T. & Stöhlker, T. (2009). Experiments on heating of low Z targets by means of hohlraum radiation. *GSI Scientif. Rept*. **2009**, 387.

Rozsnyai, B.F. (1972). Relativistic Hartree-Fock-Slater calculations for arbitrary temperature and matter density. *Phys. Rev*. **5**, 1137–1149.

Rozsnyai, B.F. (1982). An overview of the problems connected with theoretical calculations for hot plasmas. *J. Quant. Spectrosc. Radiat. Transf*. **27**, 211–217.

Sakagami, H., Johzaki, T., Nagatomo, H. & Mima, K. (2006). Fast ignition integrated interconnecting code project for cone-guided targets. *Laser Part. Beams* **24**, 191–198.

Sasaki, T., Yano, Y., Nakajima, M., Kawamura, T. & Horioka, K. (2006). Warm-dense-matter studies using pulse-powered wire discharges in water. *Laser Part. Beams* **24**, 371–380.

Shelkovenko, T.A., Pikuz, S.A., McBride, R.D., Knapp, P.F., Wilhelm, G., Sinars, D.B., Hammer, D.A. & Orlov, N.Yu. (2010). Symmetric multilayer megampere X-pinch. *Plasma Phys. Rep*. **36**, 50–66.

Shelkovenko, T.A., Sinars, D.B., Pikuz, S.A. & Hammer, D.A. (2001). Radiographic and spectroscopic studies of X pinch plasma implosion dynamics and X-ray burst emission characteristics. *Phys. Plasma* **8**, 1305–1318.

Someya, T., Miyazawa, K., Kikuchi, T. & Kawata, S. (2006). Direct-indirect mixture implosion in heavy ion fusion. *Laser Part. Beams* **24**, 359–369.

Suter, L., Rothenberg, J., Munro, D., Van Wonterghem, B., Haan, S. & Lindl, J. (1999). Feasibility of High Yield/High Gain NIF capsules. *Proc. International Fusion Sciences and Applications*. Paris: Elsevier, pp. 74–81.

Vasina, E. & Vatulin, V. (2000). Experimental scheme for investigation of ion stopping in plasma-indirect laser target design. Report No. 2000–2. Germany: GSI.

Vergunova, G.A., Guśkov, S.Yu., Rozanov, V.B. & Rosmej, O.N. (2010). Formation of plane layer of plasma under irradiation by a soft X-ray source. *J. Russian Laser Res*. **31**, 505–513.

Wilhein, Th., Rehbein, S., Hambach, D., Berglund, M., Rymell, L. & Hertz, H.M. (1999). A slit grating spectrograph for quantitative soft X-ray spectroscopy. *Rev. Sci. Instr*. **70**, 1694–1699.

Zakharov, S.M., Ivanenkov, G.V., Kolomenskii, S.A., Pikuz, S.A., Samokhin, A.I. & Ulshmid, I. (1982). Wire X-pinch in a high-current diode. *Tech. Phys. Lett*. **8**, 456–457.

Zeldovich, J.B. & Raizer, Y.P. (1966). *Phizika udarnich voln i visokotemperaturnich gidrodinamicheskich yavlenii.* M., Nauka. (in Russian).

Zou, X.B., Liu, R., Zeng, N.G., Han, M., Yuan, J.Q., Wang, X.X. & Zhang, G.X. (2006). Apulsed power generator for x-pinch experiments. *Laser Part. Beams*. **24**, 503–509.

Zschornack, G., Musiol, G. & Wagner, W. (1986). Dirac-Fock-Slater X-ray energy shifts and electron binding energy changes for all ion ground states in elements up uranium. *Preprint* ZfK-574, Zentralinstitut für Kernforschung Rossendorf bei Dresden.